



# Control of complex Ginzburg–Landau equation eruptions using intrapulse Raman scattering and corresponding traveling solutions

M. Facão<sup>a,\*</sup>, M.I. Carvalho<sup>b</sup>, S.C. Latas<sup>a</sup>, M.F. Ferreira<sup>a</sup>

<sup>a</sup> Department of Physics, I3N, University of Aveiro, Campus Universitário de Santiago, 3810-193 Aveiro, Portugal

<sup>b</sup> DEEC/FEUP and INESCPorto, University of Porto, Rua Dr. Roberto Frias, 4200-465 Porto, Portugal

## ARTICLE INFO

### Article history:

Received 17 August 2010

Accepted 5 October 2010

Available online 8 October 2010

Communicated by A.P. Fordy

## ABSTRACT

The eruption solitons that exist under the complex cubic–quintic Ginzburg–Landau equation (CGLE) may be eliminated by the introduction of a term that in the optical context represents intrapulse Raman scattering (IRS). The later was observed in direct numerical simulations, and here we have obtained the system of ordinary differential equations and the corresponding traveling solitons that replace the eruption solutions. In fact, we have found traveling solutions for a subset of the eruption CGLE parameter region and a wide range of the IRS parameter. However, for each set of CGLE parameters they are stable solely above a certain threshold of IRS.

© 2010 Elsevier B.V. All rights reserved.

## 1. Introduction

The complex cubic–quintic Ginzburg Landau equation (CGLE) is a generic equation that describes the emergence of spatio-temporal patterns on several physical systems, such as, certain chemical reactions [1], pulse propagation in fibers with linear and nonlinear gain and spectral filtering [2–5] or pulse generation in fiber lasers with additive pulse mode-locking or nonlinear polarization rotation [6,7]. This equation supports dissipative solitons which result from the balance of dispersion and nonlinearity but also of gain and loss. A diversity of dissipative solitons of the CGLE have already been found, both analytically [8,9] and numerically [10–14]. They include high and low amplitude pulse solutions, single and multi-humped pulses, solutions that travel with zero or nonzero velocity (relatively to the group velocity of the central frequency whether they exist in the optical fiber context), and also solutions with special propagation characteristics, namely, *erupting* (or *exploding*), *pulsating* and *creeping* solitons [13].

Here, we have particular interest in the erupting solitons. They have been found numerically [13] and were experimentally observed in passively mode-locked lasers [15]. Their name comes from the propagation peculiarities they exhibit: a single hump pulse propagates undistorted until it develops several side lobules that resemble an eruption, but then it recovers the original shape, in a process that repeats intermittently. These solutions exist for a relatively wide range of the CGLE parameters [13,16] and an explanation for the eruptions based on their linear stability spectrum was proposed in Ref. [17]. It turns out that certain type of opti-

cal higher order effects may be able to control these eruptions. In fact, terms similar to intrapulse Raman scattering (IRS) and self-steepening (SS) were used by Tian et al. [18] to control the eruptions, thus obtaining fixed shape soliton propagation with nonzero velocity. Also, more recently, Latas et al. [19] obtained asymmetric eruptions or complete elimination of eruptions by adding IRS, SS and third order dispersion to the CGLE.

In this Letter, we have focused in the CGLE plus IRS in order to control the eruptions. First, we used a traveling variable to reduce the partial differential equation (PDE) to a system of ordinary differential equations (ODE). These ODEs were then solved using a shooting method that searches for single hump solutions in the eruption CGLE parameter range. Finally, direct numerical simulations were performed to investigate which of those solutions have stable propagation, such that they effectively correspond to steady pulses that have replaced the CGLE eruption.

## 2. Traveling similarity variable and solutions

Let us start with the CGLE with the IRS term

$$iqz + \frac{1}{2}q_{TT} + |q|^2q = i\delta q + i\beta q_{TT} + i\epsilon|q|^2q + i\mu|q|^4q - \nu|q|^4q + T_r(|q|^2)_T q \quad (1)$$

where, in the optical context,  $q$  is the normalized envelope of the optical field, and  $Z$  and  $T$  are the normalized propagation distance and retarded time, respectively. The parameters in this equation are all normalized versions of the actual parameters, namely,  $\delta$  stands for linear gain/loss,  $\beta > 0$  for spectral filtering,  $\epsilon$  for nonlinear gain,  $\mu < 0$  for the saturation of nonlinear gain,  $\nu < 0$  for the saturation of the Kerr effect and  $T_r$  for the intrapulse Raman scattering. Note that the existence of localized pulses of the

\* Corresponding author.

E-mail address: mfacao@ua.pt (M. Facão).

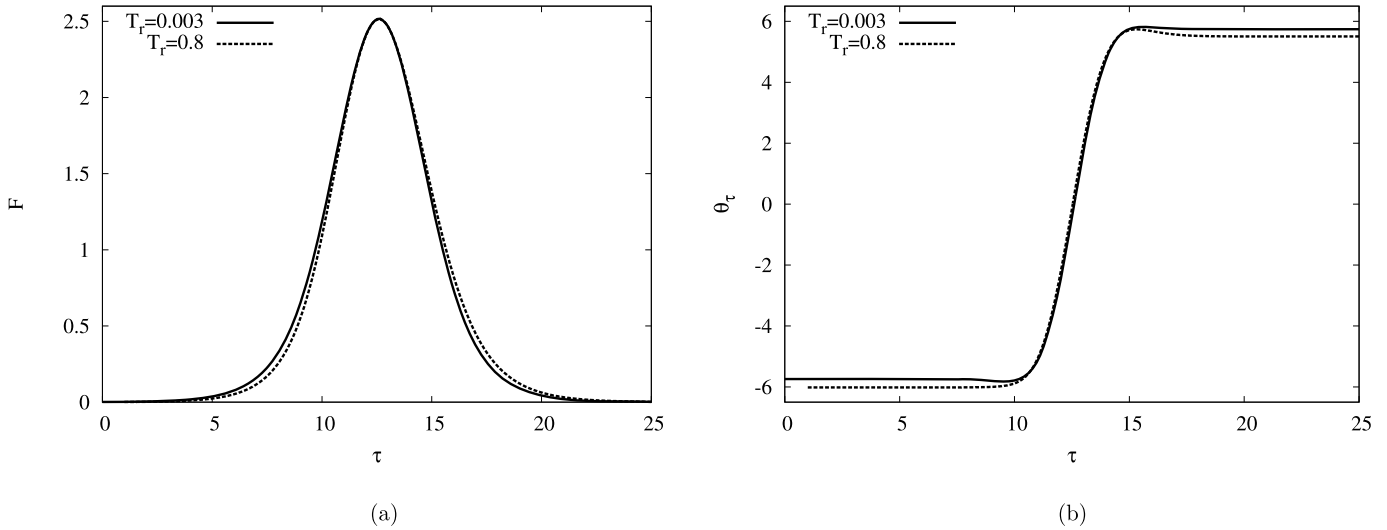


Fig. 1. (a) Amplitude profile and (b) phase derivative for  $T_r = 0.003$  and  $0.8$ .

CGLE requires that  $\delta < 0$ , such that the background waves are always eliminated, and that the nonlinear gain parameter is positive ( $\epsilon > 0$ ) [16]. Moreover, as already mentioned, erupting solitons exist for different combinations of these parameters. In this work, we will take  $\delta = -0.1$ ,  $\beta = 0.125$  and  $\mu = -0.1$ . Note that for this set of values, erupting solitons were found for a region of the parameter plane ( $v, \epsilon$ ) (see Fig. 5 of [13]).

Since we have observed stable propagation of traveling profiles with nonzero velocity when the IRS term was considered, we apply the change of variables  $q(Z, T) = F(\tau)e^{i\theta(\tau)+i\omega Z}$ , with  $\tau = T - vZ$ , where both  $F$  and  $\theta$  are real. Substitution of this envelope in the evolution equation results in

$$\begin{aligned} &\left(\frac{1}{2} + 2\beta^2\right)F'' + 2(\beta v - T_R F^2)F' + (2\beta\delta - \omega)F + v\frac{M}{F} \\ &\quad - \left(\frac{1}{2} + 2\beta^2\right)\frac{M^2}{F^3} + (1 + 2\beta\epsilon)F^3 + (v + 2\beta\mu)F^5 = 0, \\ &\left(\frac{1}{2} + 2\beta^2\right)M' + 2\beta vM - (v + 4\beta T_R F^2)FF' \\ &\quad - (2\beta\omega + \delta)F^2 + (2\beta - \epsilon)F^4 + (2\beta v - \mu)F^6 = 0 \end{aligned} \quad (2)$$

where, following the suggestion of Soto-Crespo et al. [14], we have defined  $M = F^2\theta'$  in order to obtain a system of ordinary differential equations suitable for integration. Since we are searching for localized pulses, we look for solutions such that  $F \rightarrow 0$  and  $M \rightarrow 0$  as  $\tau \rightarrow \infty$ . Then, the previous system of ODEs reduces to

$$\begin{aligned} &\left(\frac{1}{2} + 2\beta^2\right)F'' + 2\beta vF' + (2\beta\delta - \omega)F + v\frac{M}{F} \\ &\quad - \left(\frac{1}{2} + 2\beta^2\right)\frac{M^2}{F^3} = 0, \\ &\left(\frac{1}{2} + 2\beta^2\right)M' + 2\beta vM - vFF' - (2\beta\omega + \delta)F^2 = 0 \end{aligned} \quad (3)$$

which is an approximated version of (2) for small  $F$  and  $M$ . Since our numerical simulations indicate that our traveling solitons have constant phase derivative in their tails, we assume that the decaying solutions of this linear system are of the form  $F(\tau) = F_0 e^{g\tau}$  and  $M(\tau) = N_0 e^{2g\tau}$ . Note that we should have  $g$  real and positive for  $\tau \rightarrow -\infty$ , and real and negative for  $\tau \rightarrow +\infty$ , in order to

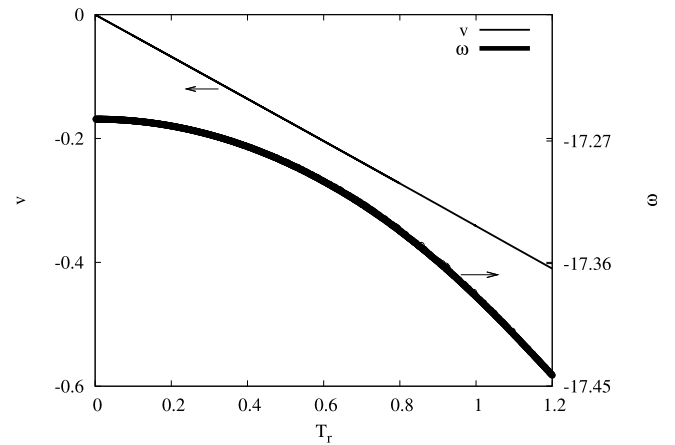


Fig. 2. Velocity and propagation constant dependence on  $T_r$  for  $\delta = -0.1$ ,  $\beta = 0.125$ ,  $\mu = -0.1$ ,  $\epsilon = 1.0$  and  $v = -0.6$ .

assure that we have real and localized solutions. Inserting these ansatz into (3) we obtain the following equations for  $g$  and  $N_0$

$$\left(\frac{1}{2} + 2\beta^2\right)g^2 + 2\beta v g - \left(\frac{1}{2} + 2\beta^2\right)\alpha^2 + v\alpha + 2\beta\delta - \omega = 0,$$

$$N_0 = \alpha F_0^2$$

where

$$\alpha = \frac{vg + \delta + 2\beta\omega}{g + 4\beta^2 g + 2\beta v}.$$

In order to obtain the single-humped solutions of (2), we planned a shooting procedure that starts from the left or right, with  $F$  and  $M$  as exponentials with real  $g$  as written above, and change  $\omega$  and  $v$  in order to obtain one hump solutions with  $F, F'$  and  $M$  small at the other tail, that is, at the right or left, respectively. However, the integration of system (2) is very sensitive to small changes in  $\omega$  and  $v$ , and the integration easily diverges or it reveals a profile  $F$  with several peaks, which correspond to the multi-humped solutions of the CGLE. Therefore, since here we are only interested in the single-humped solution, we used instead a shooting method that starts at the two tails and does the matching at the pulse peak location. The initial conditions at both ends were  $F = F_0 e^{g_{1,2}\tau} = \sigma \ll 1$ ,  $F' = g_{1,2}\sigma$  and  $M = \alpha\sigma^2$ , where  $g_1 > 0$  at the left and  $g_2 < 0$  at the right tails.

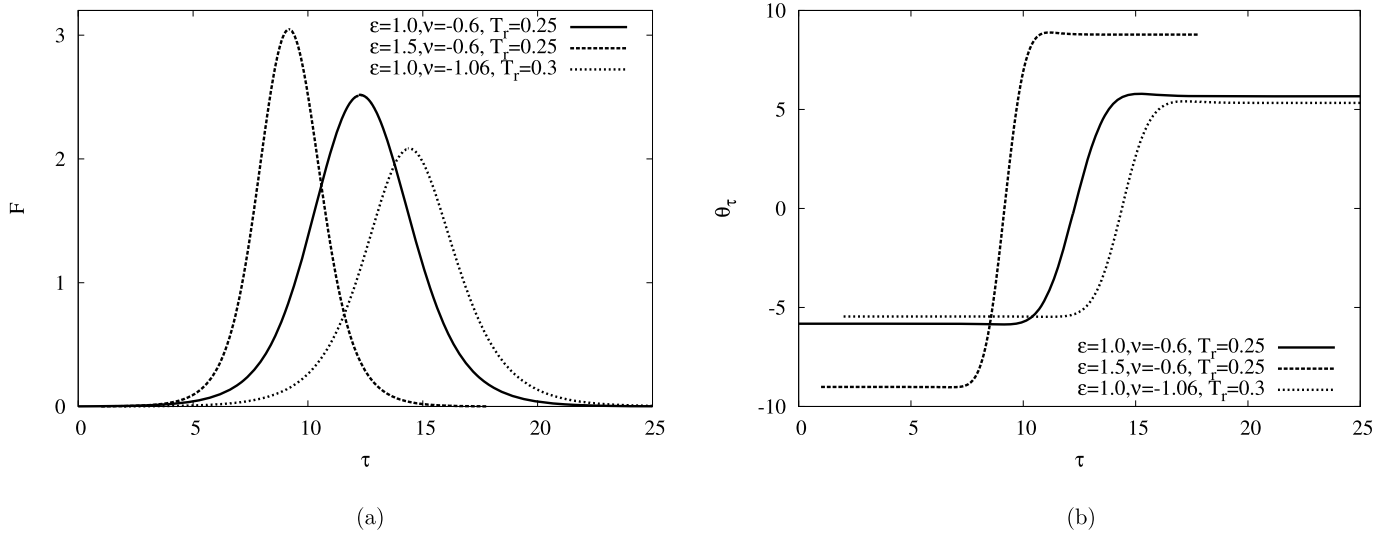


Fig. 3. (a) Amplitude profile and (b) phase derivative for  $\delta = -0.1$ ,  $\beta = 0.125$ ,  $\mu = -0.1$  and several other parameters referred on the figures.

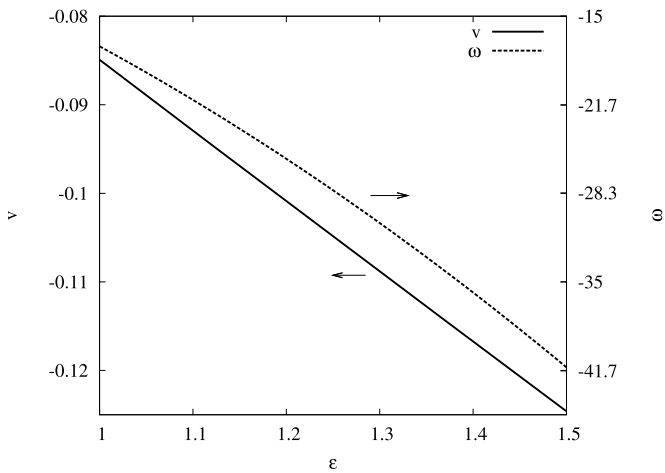


Fig. 4. Velocity and propagation constant dependence on  $\epsilon$  for  $\delta = -0.1$ ,  $\beta = 0.125$ ,  $\mu = -0.1$ ,  $\nu = -0.6$  and  $T_r = 0.25$ .

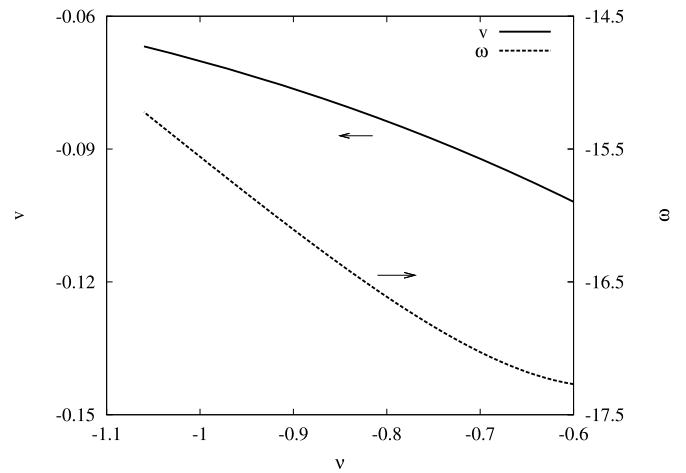


Fig. 5. Velocity and propagation constant dependence on  $\nu$  for  $\delta = -0.1$ ,  $\beta = 0.125$ ,  $\mu = -0.1$ ,  $\epsilon = 1.0$  and  $T_r = 0.3$ .

We have applied the shooting method described above and obtained single humped profiles and respective velocities and propagation constants for  $\delta = -0.1$ ,  $\beta = 0.125$ ,  $\mu = -0.1$ ,  $\epsilon = 1.0$ ,  $\nu = -0.6$  and  $T_r$  ranging from 0 to 1.2. As we increase  $T_r$ , a successful shooting was more difficult to achieve. For the values of  $T_r$  considered, the amplitude and phase profiles are reasonably identical, showing a slight asymmetry as we increase  $T_r$ . Fig. 1 shows the obtained profiles for two different  $T_r$ . The velocities vary linearly with  $T_r$  and, actually, the change in  $\nu$  is considerable (see Fig. 2). The obtained velocities are all negative, which means that the pulse is propagating in the direction of its leading edge. On the other hand, the propagation constant  $\omega$  only varies by 1% in all the considered  $T_r$  range (see Fig. 2). In fact, these traveling profiles and corresponding  $\omega$  under CGLE plus IRS are very similar to the CGLE single-humped profiles usually named SP (single-pulse). The IRS term is essentially responsible for their velocity and also a tiny asymmetry.

In our study we have restricted the search for traveling solitons to the CGLE eruptions parameter range. Therefore, in this region, the SP solutions are not stable, exhibiting the characteristic eruption behavior. However, the profile is always reappearing in between the periodic eruptions. We shall see in Section 3 at which extent the IRS effect is able to control the eruption, yielding

the propagation of a slightly asymmetric SP pulse with almost the same propagation constant but with non-zero velocity.

In order to have a wider understanding of the eruptions control by the introduction of the IRS term, we have changed  $\epsilon$  and  $\nu$  within the region of eruptions that was determined in [13]. First, we have changed  $\epsilon$  while keeping all the other previously considered CGLE parameters and choosing  $T_r = 0.25$ , and used the shooting procedure to find the corresponding profiles, velocities and propagation constants. Since our numerical PDE simulations suggest that for  $\epsilon < 1$  the explosions are controlled by a stronger IRS effect, we have only searched for profiles from  $\epsilon = 1$  up to  $\epsilon = 1.5$ , which is close to the boundary of the explosions region. The results are shown in Figs. 3 and 4. In this case, we have found profiles and  $\omega$ s that differ considerably. This result is unsurprising, since we expect that the SP profiles and  $\omega$ s for the CGLE plus IRS are close to the corresponding SP profiles of the CGLE only, which in turn show an increase of the peak amplitude and absolute value of  $\omega$  with the nonlinear gain parameter  $\epsilon$  [14].

A similar procedure has been applied for changing  $\nu$ . We have kept all other parameters as in the first experiment and changed  $\nu$  to the left of  $\nu = -0.6$ , by the same reason as above, i.e., our PDE simulations indicate that the eruptions are controlled by smaller values of  $T_r$  in that direction of  $\nu$ . The dependence of the velocity

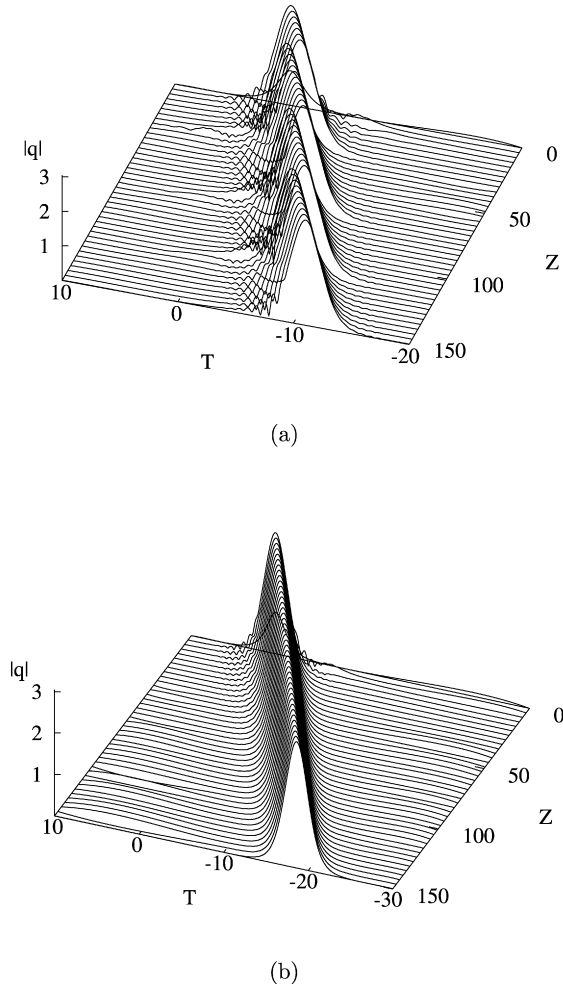


**Fig. 6.** Profile evolution under Eq. (1) for  $\delta = -0.1$ ,  $\beta = 0.125$ ,  $\mu = -0.1$ ,  $\nu = -0.6$ ,  $\epsilon = 1.5$  and (a)  $T_r = 0.2$ , (b)  $T_r = 0.25$ .

and  $\omega$  with  $\nu$  is shown in Fig. 5. Fig. 3 also shows one of the obtained profiles. In this case, the peak amplitude and the absolute value of  $\omega$  decrease as we decrease the absolute value of  $\nu$ . All these results are for  $T_r = 0.3$ .

### 3. Stability under PDE simulations

The stability of the profiles obtained in the above section, which in our study is understood as the ability of the IRS effect to control the eruptions, can be evaluated using PDE simulations. In these simulations, we have used a *sech* profile as input in order to easily excite any unstable modes that may exist. As already mentioned, we observed that, for each set of CGLE parameters within the eruption region, there is a threshold level of IRS that we need to surpass in order to achieve stable propagation. Fig. 6 shows the evolution of the profiles for  $\nu = -0.6$  and  $\epsilon = 1.5$  and two different values of  $T_r$ , one below the stability threshold and the other one above it. In this case we have obtained a threshold level of  $T_r^{\text{th}} = 0.24$ , where the threshold value means the minimum  $T_r$  for which we have observed steadily propagation of an one hump profile identical to the profile obtained in the shooting procedure. For comparison purposes, let us also refer that the threshold level for  $\epsilon = 1.0$  and  $\nu = -0.6$  is  $T_r^{\text{th}} = 0.76$ , while for  $\epsilon = 1.0$  and  $\nu = -1.06$  is  $T_r^{\text{th}} = 0.25$ . Note that in all these cases we have  $\delta = -0.1$ ,  $\beta = 0.125$  and  $\mu = -0.1$ .

In case the evolution model given by Eq. (1) is applied within the context of nonlinear pulse propagation in silica fibers, the IRS

term considered here is only an approximation of the full Raman term. According to Ref. [20], this approximation is valid for pulses that are not too short, i.e., for pulses larger than 50 fs, and the IRS non-normalized coefficient  $t_r$  is about 5 fs for silica fibers. The normalized parameter  $T_r$  is given by  $T_r = t_r/t_0$ , where  $t_0$  is the time scale used in the normalization of the time variable. Since the full-width at half-maximum (FWHM) in real and normalized times are related by  $T_{\text{fwhm}} = t_{\text{fwhm}}/t_0$ , the condition  $t_{\text{fwhm}} \geq 50$  fs implies that we should have a maximum value of  $T_r$  given by  $T_r^{\text{max}} = T_{\text{fwhm}}/10$ . As mentioned before, the normalized profiles have different FWHM as the set of CGLE parameters changes, so that we have different permitted  $T_r$  values in silica for each set. We have determined the FWHM of the three sets of CGLE parameters considered above, and calculated the maximum allowed  $T_r$  for each one. For the first set, we have  $\epsilon = 1.0$  and  $\nu = -0.6$ , and the corresponding FWHM is  $T_{\text{fwhm}} = 3.45$ . This means that, in this case, we have  $T_r^{\text{max}} = 0.345$ , which is smaller than the threshold value necessary for stable propagation. A similar scenario is obtained for the set  $\epsilon = 1.5$  and  $\nu = -0.6$ , for which we have  $T_{\text{fwhm}} = 2.07$  and  $T_r^{\text{max}} = 0.207$ , a value smaller than the threshold  $T_r^{\text{th}} = 0.24$ . A different situation occurs for the third set of values considered,  $\epsilon = 1.0$  and  $\nu = -1.06$ , which correspond to profiles with  $T_{\text{fwhm}} = 3.11$ . In this case, we have  $T_r^{\text{max}} = 0.311$  and a threshold value of only 0.25, which implies that for this set of values, eruption control can be effectively achieved by the IRS effect present in silica fibers.

### 4. Conclusions

We have observed eruptions control in PDE simulations of the CGLE whenever a term corresponding to IRS was added. Using a traveling variable, we have reduced the CGLE plus IRS to a system of ODEs which were then solved using a shooting method that searches for single-humped profiles. This numerical procedure yields profiles that resemble the single humped solution of the CGLE with the same parameters, but with a slight asymmetry. The velocities grow linearly with the IRS parameter. Moreover, the PDE simulations show that for each set of the CGLE parameters there is a value of the IRS strength above which the obtained traveling solutions are effectively stable, thus replacing the CGLE erupting solutions. Our simulations also show that, for some CGLE parameters, there is an effective control of eruptions for sufficiently large pulses such that the considered IRS approximated term is valid in silica fibers.

### References

- [1] M. Stich, M. Ipsen, A. Mikhailov, Phys. Rev. Lett. 86 (2001) 4406.
- [2] A. Mecozzi, J. Moores, H. Haus, Y. Lai, Opt. Lett. 16 (1991) 1841.
- [3] Y. Kodama, A. Hasegawa, Opt. Lett. 17 (1992) 31.
- [4] L. Mollenauer, J. Gordon, S. Evangelides, Opt. Lett. 17 (1992) 1575.
- [5] M. Matsumoto, H. Ikeda, T. Uda, A. Hasegawa, J. Lightwave Technol. 13 (1995) 658.
- [6] H. Haus, J. Fujimoto, E. Ippen, J. Opt. Soc. Am. B 8 (1991) 2068.
- [7] J. Moores, Opt. Commun. 96 (1993) 65.
- [8] N. Akhmediev, V. Afanasjev, Phys. Rev. Lett. 75 (1995) 2320.
- [9] N. Akhmediev, V. Afanasjev, J. Soto-Crespo, Phys. Rev. E 53 (1996) 1190.
- [10] V. Afanasjev, N. Akhmediev, J. Soto-Crespo, Phys. Rev. E 53 (1996) 1931.
- [11] J. Soto-Crespo, N. Akhmediev, V. Afanasjev, S. Wabnitz, Phys. Rev. E 55 (1997) 4783.
- [12] N. Akhmediev, A. Ankiewicz, J. Soto-Crespo, Phys. Rev. Lett. 79 (1997) 4047.
- [13] J. Soto-Crespo, N. Akhmediev, A. Ankiewicz, Phys. Rev. Lett. 85 (2000) 2937.
- [14] J.M. Soto-Crespo, N. Akhmediev, K.S. Chiang, Phys. Lett. A 291 (2001) 115.
- [15] S. Cundiff, J. Soto-Crespo, N. Akhmediev, Phys. Rev. Lett. 88 (2002) 73903.
- [16] N. Akhmediev, J.M. Soto-Crespo, G. Town, Phys. Rev. E 63 (2001) 056602.
- [17] N. Akhmediev, J. Soto-Crespo, Phys. Lett. A 317 (2003) 287.
- [18] H. Tian, Z. Li, J. Tian, G. Zhou, J. Zi, Appl. Phys. B 78 (2004) 199.
- [19] S. Latus, M. Ferreira, Opt. Lett. 35 (2010) 1771.
- [20] G.P. Agrawal, Nonlinear Fiber Optics, Academic Press, 2001.